frontiers | Frontiers in Forests and Global Change

TYPE Original Research
PUBLISHED 18 April 2024
DOI 10.3389/ffgc.2024.1370934

OPEN ACCESS

EDITED BY
Andrei G. Lapenas,
Albany State University, United States

REVIEWED BY
Miguel Portillo-Estrada,
University of Antwerp, Belgium
Vladan Popovic,
Institute of Forestry, Serbia

*CORRESPONDENCE
Arne Sellin
✉ arne.sellin@ut.ee

RECEIVED 15 January 2024
ACCEPTED 03 April 2024
PUBLISHED 18 April 2024

CITATION
Sellin A, Heinsoo K, Kupper P, Meier R, Õunapuu-Pikas E, Reinthal T, Rosenvald K and Tullus A (2024) Growth responses to elevated environmental humidity vary between phenological forms of *Picea abies*. *Front. For. Glob. Change* 7:1370934. doi: 10.3389/ffgc.2024.1370934

Growth responses to elevated environmental humidity vary between phenological forms of *Picea abies*

Arne Sellin[1]*, Katrin Heinsoo[1,2], Priit Kupper[1], Riho Meier[1], Eele Õunapuu-Pikas[1], Taavi Reinthal[1], Katrin Rosenvald[1] and Arvo Tullus[1]

[1]Institute of Ecology and Earth Sciences, University of Tarty, Tartu, Estonia, [2]Institute of Agricultural and Environmental Sciences, Estonian University of Life Sciences, Tartu, Estonia

Introduction: Global warming promotes geographical variability in climate, although the trends differ for the lower and higher latitudes of the Northern Hemisphere. By the end of the current century, the climate models project an increase of up to 20–30% in summer precipitation for northern Europe, accompanied by an increase in atmospheric humidity. Information on the effects of increasing precipitation and air humidity on the performance of northern trees is scant.

Methods: We studied the effects of artificially elevated air relative humidity (RH) and soil moisture on growth, phenology and needle/shoot morphology of 5-year-old Norway spruce (*Picea abies*) saplings at the Free Air Humidity Manipulation (FAHM) experimental site in eastern Estonia. The trees were subjected to three treatments: C – control, ambient conditions; H – air humidification, mean relative humidity ~ + 5%; I – soil irrigation, precipitation +15%. Trees from pure stands were sampled from three experimental plots per treatment in 2022.

Results: The needle morphology of *P. abies* was insensitive to moderate changes in air humidity and soil water content in northern mesic conditions. In contrast, the humidity treatments significantly affected shoot size, which decreased in the following order: C > I > H. This finding indicates a certain deceleration of the development of trees' assimilating surface under elevated air humidity. The humidity manipulation did not influence the timing of bud burst, but the trees differentiated between two phenological forms – early-and late-flushing forms. Trees growing under elevated RH exhibited slower growth rates compared to trees in C and I treatments. The early-flushing trees grew faster, while the late-flushing trees performed better under increasing environmental humidity.

Conclusion: At high latitudes, the increasing precipitation and concomitant rise in atmospheric humidity counteract the enhancement of trees' growth and forest productivity predicted for boreal forests due to global warming. Given that the late phenological form of *P. abies* is more tolerant of wetter climates and less threatened by late spring frosts, it has a greater potential to adapt to regional climate trends predicted for northern Europe.

KEYWORDS

atmospheric humidity, climate change, epicuticular waxes, FAHM experiment, growth responses, needle/shoot morphology, Norway spruce, phenology

1 Introduction

Forests play a crucial role in climate change mitigation and deliver a wide range of ecosystem services. One of the biggest challenges for the world's forests is increasing tree mortality and ecosystem vulnerability induced primarily by increased temperatures and changes in precipitation patterns accompanied by forest fires and insect infestations (McDowell and Allen, 2015; Venäläinen et al., 2020). In fact, global warming boosts geographical variability in climate, whereas trends are different for lower and higher latitudes of the Northern Hemisphere (Diffenbaugh and Field, 2013; IPCC, 2021).[1] The increase in global surface temperature leads to rising lower tropospheric water vapor content, specific humidity and precipitation (Dessler and Davis, 2010; Byrne and O'Gorman, 2018), with the moisture-holding capacity of the atmosphere increasing at a rate of ~7% per 1°K according to the Clausius–Clapeyron equation. By the end of the current century, the models have projected an increase of up to 20–30% in summer precipitation for northern Europe (Scoccimarro et al., 2015; see text footnote 1, respectively) and 15–19% for Estonia (Luhamaa et al., 2015).

In addition to the projected increase in specific humidity, air relative humidity (RH) increases due to the rising amount and frequency of rainfall at the local scale (Betts et al., 2014; Busuioc et al., 2016; Fanourakis et al., 2020). The RH in a warm season increased up to 10% per decade in northern Europe, Asia and some regions of Canada from 1979 to 2014 (Vicente-Serrano et al., 2018). The rising rainfall frequency will make foliage frequently wet, maintaining a high RH much longer inside the forest canopies due to the evaporation of intercepted water (Geiger et al., 2009; von Arx et al., 2012; Fanourakis et al., 2020). Mature Norway spruce (*Picea abies*) stands intercept 44–47% of the gross rainfall (Šrámek et al., 2019), and the central zone of the crowns intercepts up to 71% (Bartík et al., 2016), from where it eventually evaporates back to the atmosphere, increasing the RH on local and regional scales (Bonan, 2010). A higher RH and lower temperature combined, which is common in *P. abies* stands (Modrzyński, 2007), translate into a lower air vapor pressure deficit (VPD) within forest canopies. The role of RH in climate change has been underestimated, as trends in evapotranspiration are primarily expected to be driven by atmospheric temperature. Xiao et al. (2020) indicated that RH is still a more important driver of terrestrial evapotranspiration than temperature.

The increasing precipitation will raise the soil water content, which may cause soil hypoxia in spring and rainy periods in summer, thus affecting tree growth and carbon pools and fluxes in boreal and hemiboreal forests. The mean soil water content in summertime has significantly increased in northern Europe since the 1950s, and this trend will likely continue in the future (European Environment Agency, 2016; Xiao et al., 2020). At the same time, the climate will become more uneven, and the frequency of drought episodes is expected to increase also in northern Europe despite the increase in mean precipitation (Venäläinen et al., 2020). Soil moisture supply and VPD independently affect vegetation productivity and water use during periods of hydrologic stress (Jung et al., 2010; Park Williams et al., 2013; McDowell and Allen, 2015). Differential effects of air humidity *vs* soil moisture on plant abundance, distribution and performance have been experimentally demonstrated for both woody and herbaceous species (Lendzion and Leuschner, 2008; Leuschner and Lendzion, 2009). Thus, in addition to soil moisture, air humidity is an essential abiotic factor to consider when discussing how trees will respond to climate change and how to optimize silvicultural measures in this context. Disentangling the impact of these two critical drivers on ecosystem carbon and water cycling is challenging because they are often tightly correlated, and experimental tools for manipulating VPD in the field are scanty (Beier et al., 2012).

One of the climate change-induced trends at high latitudes is a retreat of boreal forests northward and replacement of conifers by broadleaved species driven by diverse abiotic and biotic factors (Boisvert-Marsh et al., 2014; Lindner et al., 2014; Reich et al., 2022). Model predictions suggest that the same trend holds for *P. abies*; its climatic range limit is moving northwards (Bradshaw et al., 2000; Koch et al., 2022). In general, conifers are physiologically less plastic than broadleaved species with respect to water availability (Zhang et al., 2018), and the risks ensuing from climate change are expected to be higher for coniferous than for deciduous forests, largely because of the disparity in hydraulic traits (Liu et al., 2017). Previous findings indicate that the combined effect of air humidity and soil moisture on trees' water relations, nutrient uptake and growth is hardly predictable and depends on the direction and severity of these two environmental drivers. Further increases in atmospheric humidity under a moderately humid climate, characteristic of northern Europe, tend to reduce growth rates in fast-growing deciduous tree species with sufficient soil water availability (Sellin et al., 2017; Tullus et al., 2017; Oksanen et al., 2019). *Picea abies*, a key species in northern Europe, is sensitive to drought episodes and will be threatened by future dryer and warmer climates in the southern part of its distribution area (Neuner et al., 2015; Marozas et al., 2019). Although extending the growing season due to climatic warming is expected to enhance growth in the northern forests (Mäkinen et al., 2018), the growing conditions may become suboptimal for Norway spruce, even in southern Finland (Venäläinen et al., 2020). Increasing temperatures have been shown to reduce stem diameter growth, net photosynthesis and stomatal conductance in spruce (Kivimäenpää et al., 2013, 2017). However, there is still no information on how *P. abies* will respond to the increasing precipitation and atmospheric humidity predicted for high latitudes.

Climate changes lead to a lengthening of the growth period, primarily due to shifts in spring phenophases (Menzel et al., 2006). In boreal deciduous tree species, climate warming causes an advancement in the timing of the earliest phenophases (*Betula pubescens*; Pudas et al., 2008), while increasing air humidity delays leaf senescence and autumnal foliage fall (*Betula pendula*; Godbold et al., 2014). In *P. abies*, the impact of climate change is manifested in pollination 4–8 days earlier in the last decades compared to the previous period and in shortening of the phenophase (Škvareninová and Mrekaj, 2022). Precipitation does not have a significant effect on the timing of spruce pollination.

The adaptation of forests to the future climate should be a major challenge for forest management in Europe in the coming decades (Petr et al., 2015; Luyssaert et al., 2018). Currently, knowledge of the acclimation potential of boreal tree species to a wetter climate is limited and does not allow for science-based decisions on the future organization of sustainable multifunctional forest management. The

1 https://www.eea.europa.eu/

aim of this study was to (i) analyze the growth responses of Norway spruce saplings to environmental humidity treatments (control, air humidification and soil irrigation) and (ii) assess the role of concurrent changes in spring phenology and shoot morphology in these responses.

2 Materials and methods

2.1 Experimental site and environmental conditions

The experiment was conducted at the Free Air Humidity Manipulation (FAHM) site located in eastern Estonia (58°14′ N 27°17′ E), in the northern part of the temperate zone and in the transition zone between maritime and continental climates. This site belongs to the hemiboreal forest zone, with a growing period lasting 175–180 days, from mid-April to October. The long-term mean annual precipitation in this region is 673 mm; the mean air temperature is 18.0°C in July and −4.1°C in January. The soil type at the site is fertile Endogleyic Planosol (WRB).

The FAHM facility has been established to study the effects of increasing precipitation and atmospheric humidity on tree growth and the functioning of forest ecosystems. The facility consists of nine hexagonal experimental plots (∅ 14 m) planted in the spring of 2020 with 3-year-old nursery-grown Norway spruce [*Picea abies* (L.) H. Karst.] and 2-year-old nursery-grown silver birch (*Betula pendula* Roth) trees at 1 × 1 m spacing, and surrounded by a buffer zone consisting of hybrid aspen (*Populus tremula* L. × *P. tremuloides* Michx.) trees. In each plot, ¼ represents a pure stand of *P. abies* (33 trees), ¼ – a pure stand of *B. pendula*, and ½ – a spruce–birch mixed stand. Three of the nine plots stand for the control (C) with ambient conditions. In three plots (H), the mean RH is elevated on average by 5% compared to the ambient air applying a computer-controlled system of mist emitters (button-type misting nozzles; Mist Cooling Inc., Brookshire, TX) that produce ~10-μm water droplets that evaporate instantly. Three plots are irrigated (I) by adding 15% of actual precipitation weekly using an aboveground drip irrigation system (Gardena GmbH, Ulm, Germany). The original description of the site and experimental setup are given in Kupper et al. (2011). In all experimental plots, air temperature (T_A; °C) and RH (%) were continuously recorded with shielded HMP45A humidity and temperature probes (Vaisala, Helsinki, Finland), three sensors per plot, and soil water potential at a depth of 15 cm (Ψ_{S15}) with EQ3 equitensiometers (Delta-T Devices, Burwell, United Kingdom), four sensors per plot. Rainfall was measured with an ARG100 tipping-bucket rain gage (Environmental Measurements Ltd., Sunderland, United Kingdom). The readings of the sensors were collected every 60 s and stored as average values every 10 min with data loggers (GP2 data loggers; Delta-T Devices). Air vapor pressure deficit (VPD; kPa) was calculated from T_A and RH according to Bolton (1980).

The current study was carried out on 5-year-old Norway spruce saplings in pure stands. Sample trees were randomly selected, avoiding the edges of the pure stand quarters. The summer of 2022 was relatively rainy in this region; there was 102 mm (147% of multiannual mean) of precipitation in June, 46 mm (91%) in July and 99 mm (128%) in August. Relevant environmental characteristics are presented in Figure 1 and Table 1.

2.2 Phenological observations

The spring phenology of four sample trees per plot (36 trees in total) was steadily monitored in 2022. The sample trees were selected from the central part of the pure *P. abies* stand in each plot. The top shoot and a south-facing branch belonging to the second whorl from the treetop were monitored at 2-day intervals. The day of flushing of the top bud and the day when at least three buds of the sample branch had been flushed were recorded. Flushing was defined as the moment when new needles extended at least 5 mm over the bud scale. Thereafter, elongation of the top shoot and leader shoot of the branch were recorded at weekly intervals. Growth cessation was defined as the date prior to which the last notable elongation growth (>3 mm week^{-1}) took place. Growth period of each sample tree was determined as the number of days from flushing to growth cessation. Phenological observations were carried out from mid-May to mid-July.

Due to the evident distinction between the trees in bud break times, we differentiated two phenological forms based on effective temperature sums (ETS; threshold +5°C) accumulated by the day of bud break (t_{bb}). The summation began when the daily average temperature (T_{avg}) steadily exceeded +5°C (Etverk, 1968), i.e., 18 April 2022:

$$\mathrm{ETS} = \sum_{t_0}^{t_{bb}} T_{\mathrm{avg}} - 5$$

where t_0 is the starting day for the temperature sum accumulation. According to Etverk (1968), the criteria to distinguish the phenological forms were: ETS = 133 ± 18°C and 203 ± 26°C for early-and late-flushing spruces, respectively.

2.3 Growth trait measurements

The growth traits of all *P. abies* trees in the FAHM plots were measured annually after the end of the active growth period. Tree height (H_T, cm) was recorded using an extendable measuring pole. The stem diameter at 30 cm above the ground (D_{30}, mm) was measured in two perpendicular directions with a CD-P15P digital caliper (Mitutoyo Corp., Japan). Total and relative (%) growth increments were estimated based on growth data for 2021 and 2022.

Seasonal growth dynamics of spruce stems were monitored using nine dendrometers (DD-S2, Ecomatic GmbH, Dachau, Germany) recording diameter change (μm) in 10-min intervals for three trees per treatment. Based on the daily average diameters, the relative growth increment (RGI, μm^2 μm^{-2}) of the stem basal area was estimated as follows:

$$\mathrm{RGI} = \frac{\mathrm{BA}_t - \mathrm{BA}_{t-1}}{\mathrm{BA}_{t-1}}$$

where t is the time in days, and BA_t is the stem basal area (μm^2) at time t. The dendrometric measurements were conducted from the beginning of May until the end of September (19–38 weeks of the year). To ascertain the effects of environmental factors (air temperature, T_A; air relative humidity, RH; soil volumetric water

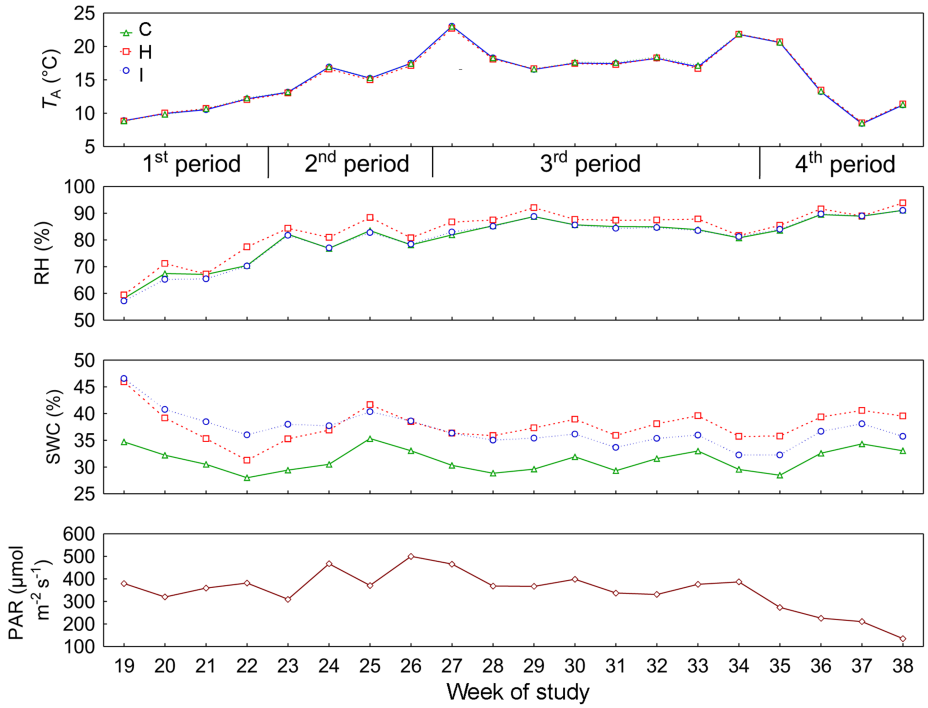

FIGURE 1
Daily means of environmental factors (T_A, air temperature; RH, air relative humidity; SWC, soil volumetric water content; PAR, photosynthetically active radiation) in different treatments: C – control, H – air humidification, I – soil irrigation. PAR indicates the conditions above the experimental plots. According to the weekly dynamics of stem relative growth increment (RGI), the whole study period was divided into four subperiods: 1st period (19–22 weeks), 2nd period (23–26 weeks), 3rd period (27–34 weeks) and 4th period (35–38 weeks).

content, SWC; photosynthetically active radiation, PAR) on the daily variability of RGI, a stepwise forward multiple regression analysis was conducted. According to the dynamics of RGI, the entire study period was divided into four subperiods for the regression analysis.

2.4 Morphometric analysis

For morphometric analysis, we sampled five trees from each experimental plot, with one current-year shoot per tree and 15 shoots per treatment in total. The most distal lateral shoots were taken from the second whorl from the treetop. Altogether, 45 shoots (3 treatments × 3 plots × 5 trees) were analyzed. To obtain the shoot silhouette area (A_{silh}), the shoots were set horizontally on a light table in a dark room and photographed with a Canon EOS 600D digital camera (Canon Inc., Tokyo, Japan) using backlighting (Ishii et al., 2012). Thus, the shoot inclination angle (φ) relative to the projection plane was 0°. The photos were taken using monochromatic mode and saved as 8-bit grayscale images. A_{silh} was measured using a WinSEEDLE (Regent Instruments Inc., Quebec, Canada) image analysis system.

After photographing the shoots, all needles were detached from the shoot axis and the width (W) and height (H_N) of 10 needles per shoot were measured manually using a micrometer. All needles were laid flat without overlap on the tray and scanned with WinSEEDLE, and the images were analyzed with the image analysis system. To estimate the surface area (A_S) and volume (V) of the needles, shoot-specific H_N/W ratios were used based on manual measurements. For A_S and V measurements, two algorithms were applied – rectangular and ellipsoidal object methods. As the rectangular approximation most likely overestimates and the ellipsoidal approximation rather underestimates the real measures (Sellin, 2000), we used the means of the two methods in the data analysis. In the present case, the ellipsoidal method resulted in an average of 17.7% lower values of A_S than the rectangular method. Both algorithms consider needle taper by slicing the needle into cross-sections perpendicular to the curved length, with each section one pixel in length. The surface area and volume of the sections were estimated and totalled to determine the needle A_S and V. Finally, all needles and shoot axes were oven dried at 80°C to a constant weight to obtain needle (M_N) and shoot axis dry masses (M_{ax}).

Based on the measurements, the following traits characterizing needle packing were calculated: needle density (ND, cm^{-1}) – number of needles per shoot axis unit length (l_{ax}); needle area packing (A_{S_T}/l_{ax}, cm^2 cm^{-1}) – total surface area of needles expressed per shoot axis unit length; shoot silhouette area to total needle area ratio (STAR). For Norway spruce shoots, A_{silh} attains its maximum value at φ = 0°, thus resulting in a maximum STAR (Palmroth et al., 2002). In addition to needle packing, STAR is a measure of light interception efficiency. Light interception per unit needle area of a conifer shoot in a given light environment is directly proportional to its shoot silhouette to total needle area ratio (Stenberg et al., 2001). In addition, some other functional traits were calculated: leaf mass per area (LMA, g m^{-2}) based on surface area, leaf mass fraction of the shoot (LMF), shoot mass per shoot silhouette area (SMA, g m^{-2}) and needle tissue density (NTD, g cm^{-3}).

TABLE 1 Means (±SE) of environmental factors recorded at the FAHM site in summer months of 2022.

Factor	Month	Treatment		
		C	H	I
Daytime* air temperature, T_A (°C)	June	21.6 ± 0.05^a	20.9 ± 0.07^b	21.4 ± 0.05^c
	July	21.9 ± 0.04^a	21.4 ± 0.06^b	21.9 ± 0.05^a
	August	24.0 ± 0.04^a	23.8 ± 0.06^b	24.2 ± 0.04^c
Daytime air relative humidity, RH (%)	June	65.8 ± 0.18^a	70.9 ± 0.14^b	66.2 ± 0.17^a
	July	70.0 ± 0.15^a	74.2 ± 0.13^b	70.2 ± 0.14^a
	August	68.2 ± 0.19^a	70.7 ± 0.19^b	68.5 ± 0.18^a
Midday** air relative humidity, RH_{md} (%)	June	61.8 ± 0.36^a	66.9 ± 0.29^b	61.7 ± 0.34^a
	July	65.6 ± 0.27^a	70.9 ± 0.26^b	65.6 ± 0.26^a
	August	62.2 ± 0.34^a	65.4 ± 0.37^b	61.7 ± 0.33^a
Daytime vapor pressure deficit, VPD (kPa)	June	0.98 ± 0.007^a	0.79 ± 0.007^b	0.94 ± 0.007^c
	July	0.85 ± 0.006^a	0.74 ± 0.007^b	0.85 ± 0.006^a
	August	1.05 ± 0.008^a	0.98 ± 0.011^b	1.05 ± 0.008^a
Midday vapor pressure deficit, VPD_{md} (kPa)	June	1.14 ± 0.016^a	0.91 ± 0.016^b	1.12 ± 0.016^a
	July	1.03 ± 0.011^a	0.84 ± 0.014^b	1.03 ± 0.014^a
	August	1.32 ± 0.016^a	1.23 ± 0.023^b	1.36 ± 0.016^a
Soil water potential at 15 cm, Ψ_{S15} (kPa)	June	−1.7 ± 0.03^a	−1.0 ± 0.00^b	−1.2 ± 0.01^b
	July	−8.8 ± 0.16^a	−1.3 ± 0.02^b	−6.2 ± 0.08^c
	August	−10.7 ± 0.16^a	−3.4 ± 0.06^b	−10.6 ± 0.12^c

*9:00–18:00 h. **12:00–14:00 h. The treatments: C – control, H – air humidification, I – soil irrigation. The superscripts indicate significant ($p < 0.001$) differences between the treatments within a month as tested with multiple comparisons of mean ranks for all groups.

To determine the number of stomatal rows (N_{SR}) and stomatal density (SD, mm^{-2}), a lateral current-year shoot from the northern side of the second whorl from the treetop of each sample tree was cut in January 2023 and kept in the freezer at −8°C until analysis. Ten needles from the central part of the shoots were detached, laid flat, and fixed at both ends with thin Scotch tape inside the diapositive frame, leaving open space for measurements. Both N_{SR} and SD were counted from a 2 mm central section under 10× magnification using a pre-calibrated stereo microscope DZ.1100 (Euromex, Arnhem, The Netherlands). The digital images were generated by ImageFocus Alpha software and saved for further analysis in jpg format. If the images of all 10 needles were saved, the frame was turned over to sample the other surface of the needles. The width of the needles was measured and SD was calculated based on the sum of stomata on both surfaces. N_{SR} was counted from the same needle images and expressed as a mean per one needle surface; incomplete rows were assigned a value of 0.5 (Wang et al., 2019). The morphological traits of the needles and shoots are listed in Table 2.

To estimate the coverage and condition of the epicuticular waxes on the epistomatal areas, five needles from the central part of the shoot were sampled. Images of the wax structure both in the stomatal antechamber and on the cuticle around the stomata were obtained with an EVO LS15 scanning electron microscope (Carl Zeiss Microscopy GmbH, Jena, Germany) in random order after the needles were fixed to aluminum specimen stubs with double-stick tape and sputter-coated with gold. To minimize the effect of temperature on waxes, the coating time was kept as short as possible. For further estimations, at least 10 images of stomata with the most structured epicuticular wax from each needle (in total 2,280 images) were taken at 2800–3500× magnification. The proportion of the original crystalline structure of epicuticular wax on the stomatal cavity was estimated by defining five distinct classes according to Trimbacher and Egkmüllner (1997): 1 – all visible wax on the stomatal antechamber surface is in tubular form; 2 – up to 25% of the epistomatal area is covered with fused or plate-like wax particles; 3 – 25 – 50% of stomatal antechamber area is covered by the degraded wax structures mentioned above; 4 – 50 – 75% of stomatal antechamber area is covered by degraded wax structures; 5 – the area of crystalline wax structure on stomatal antechamber is less than 25% or missing (Supplementary Figure S1). In the inter-stomatal areas, the typical wax structure was classified into three categories: I – tubular tufts or granules cover more than 50% of the cuticle surface; II – wax tubules or granules on the cuticle are rare; III – wax structures on the cuticle are missing or form mainly plate-like amorphous conglomerates.

2.5 Leaf chemical analysis

To estimate the nutritional status of the trees, two composite needle samples were collected from the pure *P. abies* stand quarter from each plot in mid-July 2022. One composite sample contained current-year needles from five trees taken from a branch belonging to the second whorl from the top. The needles were dried at 60°C in a desiccator for 24 h. The contents of total nitrogen (N; modified Kjeldahl method), total phosphorus (P; ICP-AES) and total potassium (K; ICP-AES) were determined by the Estonian Environmental Research Centre.

2.6 Data analysis

The effect of treatment on the morphological traits of needles and shoots and tree growth traits was assessed by applying a mixed-effects analysis of variance (ANOVA). The factors were: 'Treatment',

TABLE 2 Symbols and units of measurement for morphological traits used in the study.

Symbol	Trait	Unit
A_P	Needle projected area	mm^2
A_{P_T}	Total needle projected area	cm^2
A_S	Needle surface area	mm^2
A_{silh}	Shoot silhouette area	cm^2
A_{S_T}	Total needle surface area	cm^2
A_{S_T}/l_{ax}	Needle area packing	$cm^2\ cm^{-1}$
H_N/W	Needle height to width ratio	–
l_{ax}	Length of shoot axis	cm
l_N	Needle length	mm
LMA	Leaf mass per area	$g\,m^{-2}$
LMF	Leaf mass fraction of the shoot	–
M_{ax}	Shoot axis dry mass	g
M_N	Total needle dry mass	g
ND	Needle density	cm^{-1}
N_N	Number of needles	–
N_{SR}	Number of stomatal rows	–
NTD	Needle tissue density	$g\,cm^{-3}$
SD	Stomatal density	mm^{-2}
SMA	Shoot mass per shoot silhouette area	$g\,m^{-2}$
STAR	Shoot silhouette area to total needle area ratio	–
V	Needle volume	mm^3
W	Needle width	mm

'Experimental plot' (nested in the former) and 'Phenological form'. 'Experimental plot' was treated as a random factor. For analysis of the phenological growth dynamics, we introduced an additional factor 'Calendar week' into the analysis model. The models included both main and interaction effects of the factors. The normality of the data and the homogeneity of variances were checked using Lilliefors and Levene's tests, respectively. The model residuals were inspected visually from residual plots (histogram, Q-Q plot). When necessary, we applied logarithmic or complex transformations to the data. *Post hoc* mean comparisons were conducted using Tukey's honestly significant difference (HSD) test. The incidence of epicuticular wax categories in different treatments was analyzed using non-parametric Kruskal–Wallis ANOVA, followed by a median test. Principal component analysis (PCA) was used to condense needle/shoot morphological and tree growth traits into several principal components and to determine the particular traits contributing to these components. The PCA included 45 observations (15 per treatment), with 34 variables in total. The first three principal components explained 59% of variance in the data and were used in the subsequent analysis.

Bivariate relationships between the focal traits and independent variables were assessed by applying Pearson correlation analysis and simple linear or non-linear regression procedures based on the least squares method. Statistical data analyses were carried out using Statistica Vers. 7.1 (StatSoft Inc., Tulsa, OK) and R software packages lme4, lmerTest and emmeans (R Core Team, 2018). In all analyses, significance in statistics was evaluated at $p < 0.05$.

3 Results

3.1 Growth, phenology and leaf nutritional status

The majority of the growth traits were affected by the interaction of humidity treatment and phenological form, with the exception of H_T, which was 23% lower in H treatment compared to C treatment irrespective of the phenological form (Tables 3, 4). The raw data on tree growth can be found in Supplementary Table S1. In early-flushing spruces, three growth traits (ΔH_T, relative ΔH_T and D_{30}) had significantly lower means in H than in C treatment. The growth of the late-flushing form did not differ between the C and H treatments. Growth traits in the I treatment did not differ from those in C; hence, the differences between I and H were similar to those revealed between C and H treatments. The growth difference between the two phenological forms occurred primarily in the H treatment, where late-flushing spruces showed greater growth rates than early-flushing spruces. In contrast, early-flushing spruces had greater means of relative ΔH_T and relative ΔD_{30} in the C treatment and greater relative ΔH_T, D_{30} and ΔD_{30} in the I treatment. The stem slenderness (H_T:D_{30} ratio) of late-flushing spruces was lower in the H treatment than in other treatments.

The spring phenology of spruces mainly depended on the phenological form, but we did not detect any significant impact of the humidification or irrigation treatment. The average DOYs of bud burst of the branches were 142 (22 May) and 153 (2 June) in the early-and late-flushing trees, respectively (Table 5). Bud burst of the top shoot occurred 1–3 days later. Bud burst occurred at about 37% lower ETSs in early- than in late-flushing spruces (Table 5). The average DOYs of branch and top shoot growth cessation were 175 and 185 in early-flushing spruces and 185 and 190 in late-flushing spruces, respectively. The growth of the top shoot lasted 4 days longer in early-flushing trees, but the branch growth period did not differ between the phenological forms. The total increment of the top shoot was inversely correlated with the date of bud burst (Figure 2). Such a trend was not observed in the branches.

No significant differences ($p > 0.05$) between the treatments were observed in stem RGI during the study period (Figure 3). During the first 4 weeks (19–22 weeks), the RGI demonstrated a continuous increase, whereas a sharp decrease in RGI occurred in the second (23–26 weeks) and fourth (35–38 weeks) subperiods. Regression analysis (Tables 6, 7) revealed that the variability in the RGI during the first subperiod was mainly driven by the air temperature increase (Figure 1). In the second subperiod, the decrease in RGI was best described by the increase in SWC (C and H treatments) and RH (I treatment). PAR mainly described the variability in RGI in the third subperiod. Similarly to the second period, the decrease in RGI was best predicted by the SWC increase in the fourth subperiod (Tables 6, 7; Figure 1).

A comparison of the seasonal shoot elongation dynamics of the two phenological forms (Supplementary Figure S2) revealed that the growth of the top shoot was greater in early-flushing spruces during weeks 23–25 and in late-flushing trees during weeks 27 and 28 (Form

TABLE 3 Comparison of growth and nutritional characteristics (mean ± SE) of trees in different FAHM treatments (C – control, H – air humidification, I – soil irrigation) and different phenological forms (E – early-flushing, L – late-flushing).

Characteristics	Form	Treatment			*p*-value (Effect)
		C	H	I	
Growth traits ($n = 257$)					
H_T (cm)	E, L	121 ± 3.9^{b}	93 ± 4.1^{a}	125 ± 3.9^{b}	0.002 (Tr)
ΔH_T (cm yr.$^{-1}$)	E	34 ± 2.5^{b}	14 ± 2.8^{a}	37 ± 2.5^{b}	0.002 (Tr × F)
	L	31 ± 2.6^{ab}	$21 \pm 2.7^{a*}$	33 ± 2.7^{b}	
Relative ΔH_T (%)	E	$39.2 \pm 2.84^{b*}$	18.3 ± 3.17^{a}	$40.9 \pm 2.80^{b*}$	<0.001 (Tr × F)
	L	33.8 ± 2.96^{a}	$28.2 \pm 3.03^{a*}$	35.9 ± 3.01^{a}	
D_{30} (mm)	E	15.0 ± 0.63^{b}	11.5 ± 0.71^{a}	$16.2 \pm 0.62^{b*}$	0.005 (Tr × F)
	L	15.1 ± 0.66^{a}	$13.2 \pm 0.68^{a*}$	15.1 ± 0.68^{a}	
ΔD_{30} (mm yr.$^{-1}$)	E	4.2 ± 0.35^{ab}	2.8 ± 0.38^{a}	$5.2 \pm 0.35^{b*}$	<0.001 (Tr × F)
	L	3.9 ± 0.37^{a}	$3.8 \pm 0.37^{a*}$	4.6 ± 0.37^{a}	
Relative ΔD_{30} (%)	E	$39.1 \pm 3.06^{ab*}$	30.8 ± 3.27^{a}	46.5 ± 3.04^{b}	<0.001 (Tr × F)
	L	34.4 ± 3.14^{a}	$40.5 \pm 3.18^{a*}$	43.2 ± 3.17^{a}	
H_T:D_{30} (m cm^{-1})	E	0.81 ± 0.01^{a}	$0.79 \pm 0.02^{a*}$	0.79 ± 0.01^{a}	0.034 (Tr × F)
	L	0.81 ± 0.01^{b}	0.74 ± 0.01^{a}	0.82 ± 0.01^{b}	
Nutritional status ($n = 18$)					
Needle N content (%)	ne	1.83 ± 0.073	1.68 ± 0.073	1.83 ± 0.073	ns
Needle P content (%)	ne	0.26 ± 0.016	0.23 ± 0.016	0.23 ± 0.016	ns
Needle K content (%)	ne	0.59 ± 0.068	0.55 ± 0.068	0.49 ± 0.068	ns

Significant ($p < 0.05$) differences between the treatments (Tr) are shown with superscripts and between the forms (F) with asterisk (shown next to the higher mean value); ns – not significant, ne – not estimated.

TABLE 4 Comparison of phenological characteristics (mean ± SE) of trees ($n = 36$) in different FAHM treatments (C – control, H – air humidification, I – soil irrigation) and different phenological forms (E – early-flushing, L – late-flushing).

Characteristics	Form	Treatment			*p*-value (Form effect)
		C	H	I	
Top shoot bud burst (DOY)	E	146 ± 2.0	145 ± 2.3	142 ± 2.2	<0.001
	L	154 ± 2.2*	155 ± 2.0*	154 ± 2.0*	
Branch bud burst (DOY)	E	142 ± 1.1	142 ± 1.3	141 ± 1.3	<0.001
	L	155 ± 1.3*	152 ± 1.1*	153 ± 1.1*	
Top shoot growth cessation (DOY)	E	186 ± 1.9	185 ± 2.2	185 ± 2.2	0.001
	L	191 ± 2.3*	187 ± 1.9*	192 ± 1.9*	
Branch growth cessation (DOY)	E	176 ± 2.2	177 ± 2.6	172 ± 2.6	<0.001
	L	185 ± 2.6*	183 ± 2.2*	186 ± 2.2*	
Top shoot growth period (days)	E	39 ± 1.6*	40 ± 2.1*	43 ± 1.9*	0.002
	L	36 ± 2.1	32 ± 1.6	38 ± 1.6	
Branch growth period (days)	E, L	32 ± 1.7	33 ± 1.7	32 ± 1.7	ns
Top shoot growth rate (mm day^{-1})	E, L	7.4 ± 0.83	6.0 ± 0.83	8.5 ± 0.81	ns
Branch growth rate (mm day^{-1})	E, L	4.0 ± 0.39	4.2 ± 0.39	4.6 ± 0.39	ns

Treatment effect was not significant, significant ($p < 0.05$) differences between the forms are indicated with asterisk (shown next to the higher mean value); ns – not significant.

× Week, $p < 0.001$), the differences in the branch growth dynamics were similar (Form × Week, $p < 0.001$). We also observed a Treatment × Form × Week interaction in the growth of the top shoot ($p = 0.002$) and branches ($p = 0.008$). In early-flushing spruces, top shoot growth was higher in I than in H treatment in weeks 24 and 25 (Figure 4A). In late-flushing spruces, growth differed between the I and H treatments in week 27, and both I and C differed from the H treatment in week 28 (Figure 4B).

The treatments did not differ in the macronutrient contents of the needles (Table 3).

TABLE 5 Average day of year (DOY) and effective temperature sum (ETS) of bud burst in early- (E; $n = 17$) and late-flushing (L; $n = 19$) spruces.

Characteristics	Form	DOY (mean ± SE)	p-value (form effect)	ETS (mean ± SE)	p-value (form effect)
Top shoot bud burst	E	145 ± 1.3	<0.001	152 ± 10.6	<0.001
	L	154 ± 1.2		227 ± 9.8	
Branch bud burst	E	142 ± 0.7	<0.001	130 ± 6.2	<0.001
	L	153 ± 0.7		217 ± 6.0	

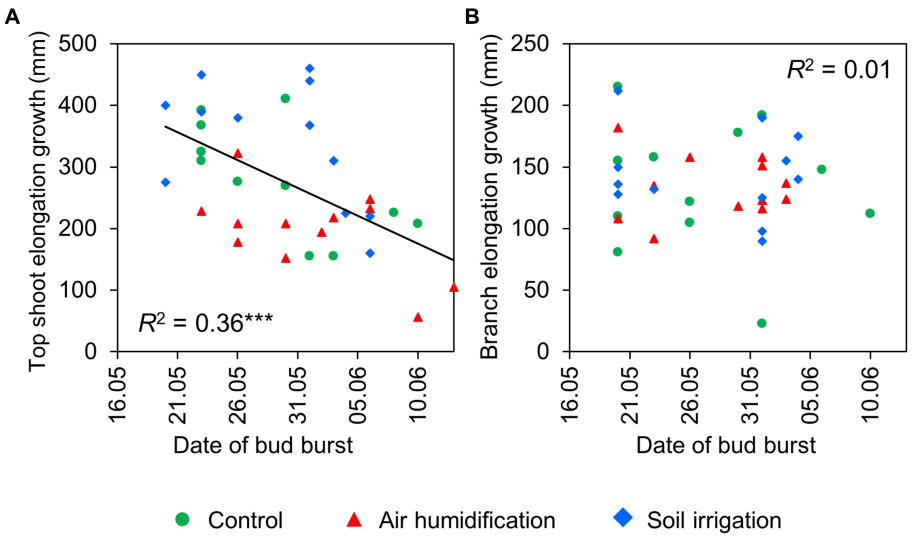

FIGURE 2
Relationship between date of bud burst and elongation growth of top shoots **(A)** and branches **(B)** in 2022.

3.2 Needle and shoot morphology

The humidity treatments had no significant effect on any morphological traits of the needles (Supplementary Table S2). The needles of spruce saplings demonstrated traits characteristic of shade foliage. The mean values (± SE) of the traits across all treatments were as follows: H_N, 0.56 ± 0.01 mm; H_N/W, 0.53 ± 0.01; and LMA, 57.5 ± 0.9 g m^{-2}. The number of stomatal rows (N_{SR}) and stomatal density (SD) did not depend on the treatment, but both varied considerably among the trees (N_{SR}, 2.6–5.6; SD, 20.4–42.4 mm^{-2}). The variation in SD was driven more by N_{SR} (semi-partial correlation $sr = 0.78$) than W ($sr = -0.69$). Shade traits were also characteristic of shoot morphology, as STAR averaged 0.255 ± 0.003 and SMA 302 ± 6 g m^{-2}.

The needle packing characteristics (ND, SMA and STAR) did not depend on humidity treatments except for needle area packing (A_{S_T}/l_{ax}). A_{S_T}/l_{ax} was significantly lower in the H treatment (3.74 cm^2 cm^{-1}) compared to the C (4.62 cm^2 cm^{-1}) and I treatments (4.21 cm^2 cm^{-1}). Variation in A_{S_T}/l_{ax} was primarily governed by A_S ($sr = 0.87$) and to a smaller extent, by N_N ($sr = 0.64$) and l_{ax} ($sr = -0.44$). As STAR can be expressed as a product of three components (Ishii et al., 2012) – LMA, LMF and SMA – we analyzed the contribution of these components to STAR. Variation in STAR was primarily determined by SMA ($sr = -0.92$), followed by LMA ($sr = 0.81$) and LMF ($sr = -0.70$). LMA, in turn, depended on NTD ($sr = 0.62$) and H/W ($sr = 0.45$), while it was invariant of A_S.

The humidity treatments did not significantly influence the condition of epicuticular waxes on the stomatal antechambers. The mean wax condition index (WCI) was 1.8 for the C and H treatments and 2.0 for the I treatment. The wax quality index also did not differ between the early- and late-flushing trees. The humidity manipulation significantly ($p < 0.001$) affected the occurrence of epicuticular waxes outside the epistomatal area (Figure 5). In the H treatment, the wax structure of category I dominated (79% of needles), while in the I and C treatments, the frequency of its occurrence was only 8–12%. The wax of category III dominated (71–74% of needles) in trees growing in C and I plots, with low occurrence (8%) in the H plots. The two phenological forms did not differ in the distribution of epicuticular waxes outside the epistomatal area. The incidence of wax categories significantly depended on needle and shoot size, tree size, and growth rate. Across all treatments, the incidence of category I wax was inversely correlated with needle size (Pearson correlation coefficient $r = -0.36 \ldots -0.42$), shoot size ($r = -0.43 \ldots -0.50$) and tree size characteristics ($r = -0.53 \ldots -0.65$) as well as with tree height and radial increments ($r = -0.39 \ldots -0.52$). In contrast, the incidence of category III wax was positively related to needle size ($r = 0.34 \ldots 0.40$), shoot size ($r = 0.34 \ldots 0.42$), tree size ($r = 0.47 \ldots 0.55$) and tree increments ($r = 0.37 \ldots 0.40$).

Unlike the needle morphological traits, all shoot size characteristics varied substantially among the treatments. The largest shoots occurred in C, followed by the I and H treatments (Figure 6; Supplementary Table S2). All traits characterizing shoot size were

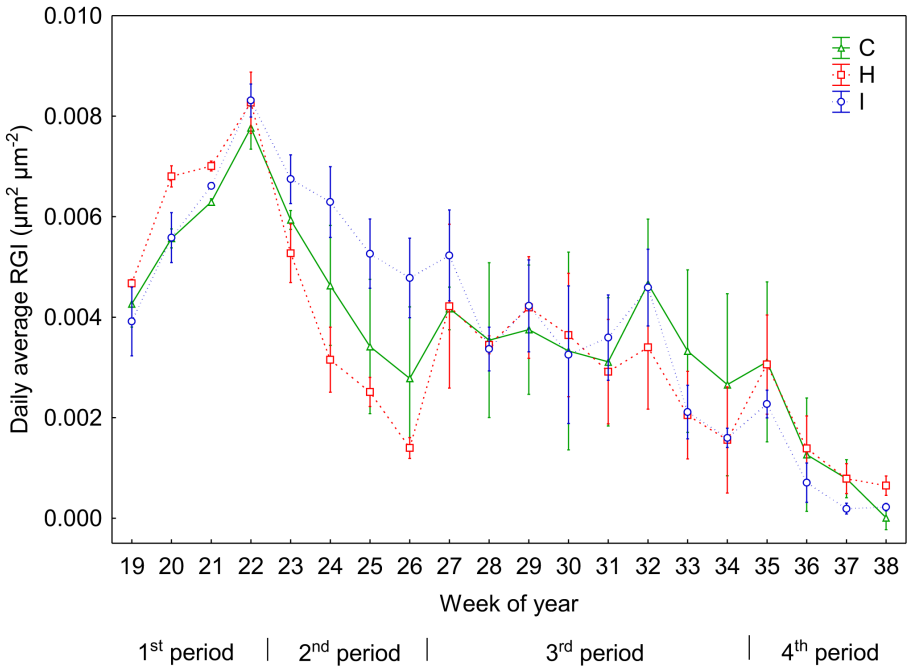

FIGURE 3
Daily means (±SE) of relative increment of the stem basal area (RGI) in three treatments during the experiment (weeks 19–38). According to the weekly dynamics of RGI, the whole study period was divided into four separate subperiods: 1st period (weeks 19–22), 2nd period (weeks 23–26), 3rd period (weeks 27–34) and 4th period (weeks 35–38).

correlated ($r = 0.38$–0.53, $p < 0.05$) with absolute height increments (ΔH_{22}) in 2022 and more weakly correlated with relative growth rate (Figure 7). Stem diameter increments (ΔD_{22}) were correlated only with M_{ax} ($r = 0.40$) and l_{ax} ($r = 0.38$).

PCA revealed that the cumulative contribution of the top three principal components that mainly governed the morphological variation of *P. abies* shoots and needles reached 58.5%, indicating that treatment had a strong impact on PC1 scores (Figure 8). PC1, corresponding to the largest eigenvalue (10.17), accounted for approximately 29.9% of the total variance. This component was primarily associated with shoot size traits with strong contribution from A_{S_T}, M_N and A_{silh}. PC2, corresponding to the second eigenvalue (5.58), accounted for approximately 16.4% of the total variance. This factor was mainly associated with needle size (A_S, A_P and V) and biomass distribution within a shoot (LMF). PC3 (eigenvalue 4.14) accounted for 12.2% of the total variance and reflected needle morphological variability (H_N, LMA and H_N/W). Along the PC1 axis, the H treatment resulted in the trait sets differing from both the trees growing in C and I plots. The last two treatments had more trees with similar characteristics, but the control trees were the most variable in terms of the traits studied. In general, H trees had shorter and lighter shoots with smaller assimilating surfaces compared to the other plots. This pattern was supplemented by the smaller height of the trees. The eigenvalues of the first three components from PCA are presented in Supplementary Table S3.

Unlike the insignificant effects of humidity treatments on needle morphology, the two phenological types differed in some morphometric traits of needles (Supplementary Table S4). The early-flushing trees exhibited a higher LMA than late-flushing trees (60.2 versus 54.4 g m^{-2}, $p < 0.001$), obviously due to a higher height to width ratio (H_N/W) and needle tissue density (NTD). Although H_N/W and NTD did not differ significantly between the phenological forms, their combined effects resulted in substantial differences in LMA. As a result of these trends, the needles of the early-flushing trees were also heavier compared to the late-flushing form; the dry weight of 1,000 needles was 1.76 and 1.48 g, respectively. The shoot size parameters did not differ between the forms, except for those associated with dry weight – M_N, M_{ax} and SMA (Supplementary Table S4).

4 Discussion

4.1 Morphological responses

Needles of spruce saplings demonstrated morphological traits characteristic of shade foliage (Sellin, 2000, 2001; Gebauer et al., 2019), although the shoots were sampled from the second whorl of the treetop, i.e., from the unshaded part of the canopy. This may be associated with spruce life history traits, specifically with the smallness and young age of the trees (Matějka et al., 2014). In addition, in the present study, we sampled the current-year needles, which are thinner, flatter, lighter and with lower LMA than older needles (Sellin, 2000). None of the needle traits were affected by the humidity treatments (Supplementary Table S2). Additionally, the traits expressing needle packing (ND, SMA and STAR) were invariant of the treatments, except for A_{S_T}/l_{ax}. However, *P. abies* is a shade-tolerant species (Modrzyński, 2007) characterized by a high morphological plasticity of needles with respect to irradiance (Sellin, 2001). The current-year and shade-grown foliage exhibits higher plasticity compared to older and well-illuminated foliage. In fact, the

TABLE 6 Results of the forward stepwise multiple regression analysis of relative growth increment (RGI) in three different treatments (C – control, H – air humidification, I – soil irrigation) in four study periods: first (weeks 19–22), second (weeks 23–26), third (weeks 27–34), fourth (weeks 35–38).

Period	Treatment	Variable	Step	R^2	R^2 change	*p* value
first	C	T_A	1	0.51	0.51	<0.001
(19–22 w)						
	H	T_A	1	0.41	0.41	<0.001
	I	T_A	1	0.59	0.59	<0.001
second	C	SWC	1	0.29	0.29	<0.01
(23–26 w)						
	H	SWC	1	0.21	0.21	<0.05
	I	RH	1	0.23	0.23	<0.05
third	C	PAR	1	0.21	0.21	<0.001
(27–34 w)						
	H	SWC	1	0.14	0.14	<0.01
		PAR	2	0.23	0.09	<0.05
	I	PAR	1	0.17	0.17	<0.01
fourth	C	SWC	1	0.36	0.36	<0.001
(35–38 w)						
	H	SWC	1	0.32	0.32	<0.01
	I	SWC	1	0.38	0.38	<0.001

The independent variables: air temperature (T_A), air relative humidity (RH), soil volumetric water content (SWC) and photosynthetically active radiation (PAR). The table does not include independent variables whose effect on RGI was not statistically significant.

morphology of the needles, shoots and crowns is strongly affected by light availability (Niinemets and Kull, 1995; Palmroth et al., 2002; Grassi and Giannini, 2005; Bednář et al., 2022).

Our results suggest that the needle morphology of *P. abies* is insensitive to moderate changes in air humidity in northern conditions, as shown in previous studies (Stenberg et al., 1999; Palmroth et al., 2002). Furthermore, soil water availability did not differ among treatments, being close to the saturation state due to the rainy summer (Table 1). The same also holds true for stomatal morphology, which is in line with a common garden experiment that revealed high physiological plasticity and low stomatal plasticity in four spruce species under manipulated humidity conditions (Wang et al., 2019). Nevertheless, in Balkan mountain forests, the needle size traits were slightly larger in the wetter climate (more precipitation), except for needle length (Popović et al., 2022), while in Swiss forests, l_N increased significantly with increasing evaporative demand (spring and summer VPD) and decreased with increasing spring precipitation and soil water availability (Zhu et al., 2022). The inconsistent morphological responses of spruce needles in mountain forests can be attributed to other environmental factors that vary with altitude and relief. Strong drought stress has been shown to reduce needle dimensions but only in portions of the canopy exposed to sunlight (Gebauer et al., 2019). The increased production of epicuticular waxes under drought conditions confirms the role of waxes in drought stress adaptation, as shown in *Pinus pinaster* (Le Provost et al., 2013).

Epicuticular wax structures on the surface of conifer needles are usually studied in the region of the stomatal antechambers. The newly formed wax crystalloids in this area degrade to more amorphous plate-like structures during needle aging, and the process can be accelerated by various external factors, including air pollution (Koppel and Heinsoo, 1996). The humidity treatments in our experiment did not have any impact on the appearance of wax in this region. However, significant differences in the epicuticular wax outlook were detected in the region between the stomata (Figure 5). This region has rarely been suggested for wax monitoring on conifers (Tuomisto, 1988) but has been found to be useful for monitoring the effect of acid mist on the needle surface (Esch and Mengel, 1998). The more aggregated epicuticular wax on the needles' surface in the humidity treatment is most likely the result of altered metabolic pathways during wax synthesis, as variable end-products form different structures on the cuticular surface (Barthlott et al., 1998). We are not sure whether such a change is

TABLE 7 Linear regression slopes of the relationship between relative growth increment (RGI) and predictor environmental variables (air temperature (T_A), air relative humidity (RH), soil volumetric water content (SWC) and photosynthetically active radiation (PAR)) in control (C), air humidification (H) and soil irrigation (I) treatments during different sampling periods (weeks of the year).

Sampling period	Predictor variable	C treatment	H treatment	I treatment
first (19–22 w)	T_A	0.0009***	0.0010***	0.0011***
	RH	ns	ns	ns
	SWC	−0.0007**	−0.0003*	−0.0005**
	PAR	ns	ns	0.00001*
second (23–26 w)	T_A	ns	ns	ns
	RH	ns	ns	−0.0002*
	SWC	−0.0004**	−0.0004*	−0.0005*
	PAR	ns	ns	0.000008*
third (27–34 w)	T_A	0.0003*	ns	ns
	RH	−0.0002**	−0.0002*	−0.0002*
	SWC	ns	−0.0005**	ns
	PAR	0.00001***	0.00001**	0.00001**
fourth (35–38 w)	T_A	0.0003**	0.0002**	0.0002**
	RH	−0.0002**	−0.0002*	−0.0002**
	SWC	−0.0006***	−0.0006**	−0.0005***
	PAR	0.00001*	ns	ns

caused by environmental drivers during shoot growth, but one can speculate that such an adaptation can be beneficial to avoid the formation of water film on the needle surface and to support photosynthetic CO_2 assimilation in humid air (Šantrůček, 2022). Possible effects of the changes in the wax structure on shoot water relations (cuticular transpiration, residual leaf conductance and surface wettability) require further study.

In contrast to the needle traits, shoot size varied significantly among the treatments in the FAHM experiment (Figure 6; Supplementary Table S2). The size of the shoots decreased in the following order: C > I > H. This trend is attributable to both a decreased number of needles and a shorter shoot axis in the humidity-manipulated plots and can be treated as a result of cumulative effects during two consecutive growing seasons. The number of needles in current-year shoots is shaped by the environmental conditions of the previous year, as the vegetative winter bud possesses all of the next year's needle primordia (Hejnowicz, 2007).

4.2 Phenology and growth

While the humidity treatment effect on the seasonal dynamics of stem RGI was insignificant (Figure 3), naturally varying environmental factors governed the trees' radial growth rate irrespective of the treatments. The relative radial growth rates were highest in May, primarily driven by the air temperature increase (Table 6). In Finland, both radial and height increments of *P. abies* have been shown to be positively related to early summer temperatures (Mäkinen et al., 2000, 2002). Keenan et al. (2014) indicated that net carbon uptake increases through temperature-induced changes in temperate forest phenology. Our results clearly revealed that early-flushing spruce trees exhibited higher growth rates at the beginning of the growing period compared to late-flushing trees (Supplementary Figure S1), but their positions changed after achieving the growth rate peak. This finding is in accord with the growth phenology reported for Central European forest trees; the earlier high growth rates are followed by a sharp drop in growth in July, whereas the later achieved growth rate peaks are sustained for a longer time (Matula et al., 2023). Across all treatments, the height increments of spruce trees were inversely related to the date of budburst (Figure 2A).

The two phenological forms of *P. abies* differed in growth traits depending on the humidity treatments. The negative effect of air humidification on growth was manifested only in the early-flushing spruce phenoform, while the growth of the late-flushing form did not differ between the treatments. Thus, the late-flushing form exhibited a better acclimattion capacity to elevated air humidity than the early-flushing form. A better tolerance of late-flushing phenological forms of climate change-related stress has also been observed in other tree species, such as *Quercus robur* (Utkina and Rubtsov, 2017) and *Fagus sylvatica* (Arnič et al., 2021). In *P. abies*, the onset and cessation of radial and height increments are independent phenomena, both contributing to forest productivity via the duration of the growing period (Mäkinen et al., 2018). Thus, earlier bud burst should support greater growth; however, a strong positive correlation observed between bud burst and frost damage (Lundströmer et al., 2020) indicates that earlier bud burst increases the risk of damage from late spring frost. For comparison, the trees of *Picea mariana* showing an early bud flush also exhibited early reactivation of xylem differentiation, but they did not differ in radial increments from late-flushing trees (Perrin et al., 2017).

After achieving a peak in the 22nd week, the RGI declined until the 26th week. This decline coincided with the highest rate of tree height growth. It is probable that the intense growth of shoots led to a decline in stem radial growth rate, as a strong incentive is given

10.3389/ffgc.2024.1370934

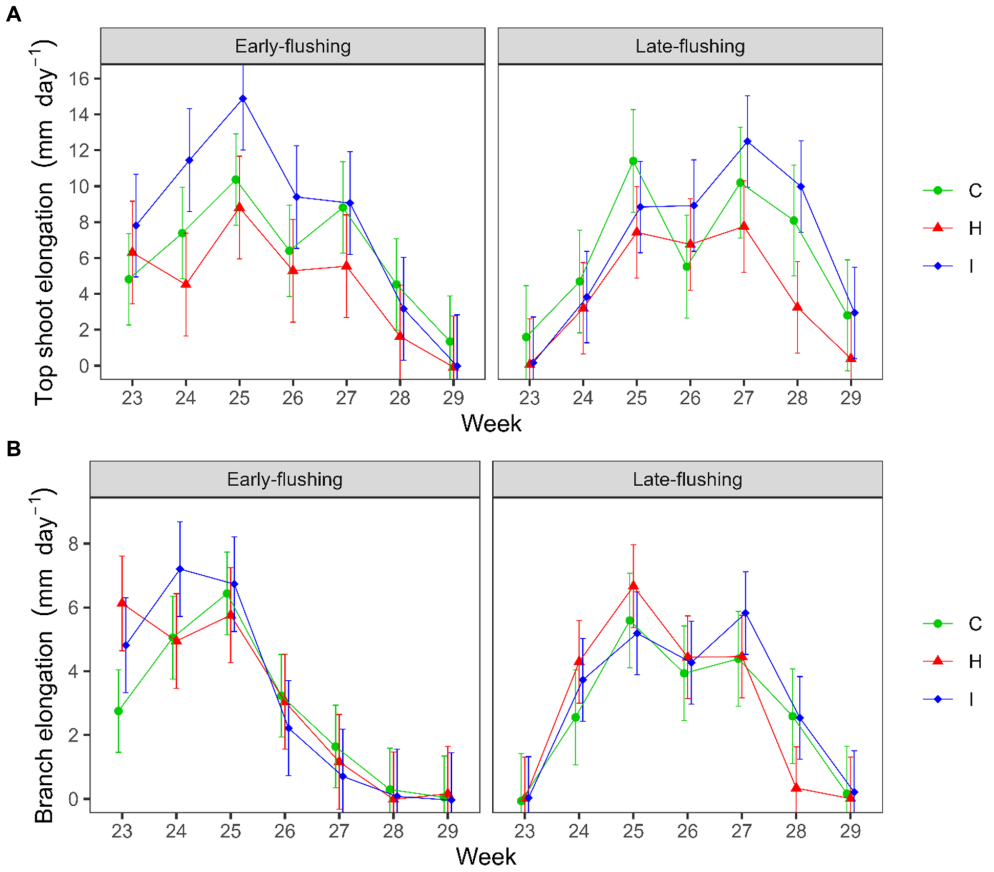

FIGURE 4
Weekly dynamics of the **(A)** top shoot and **(B)** branch elongation rate of early-and late-flushing spruces in the FAHM treatments (C – control, H – air humidification, I – soil irrigation). Error bars show 95% confidence intervals for the weekly means.

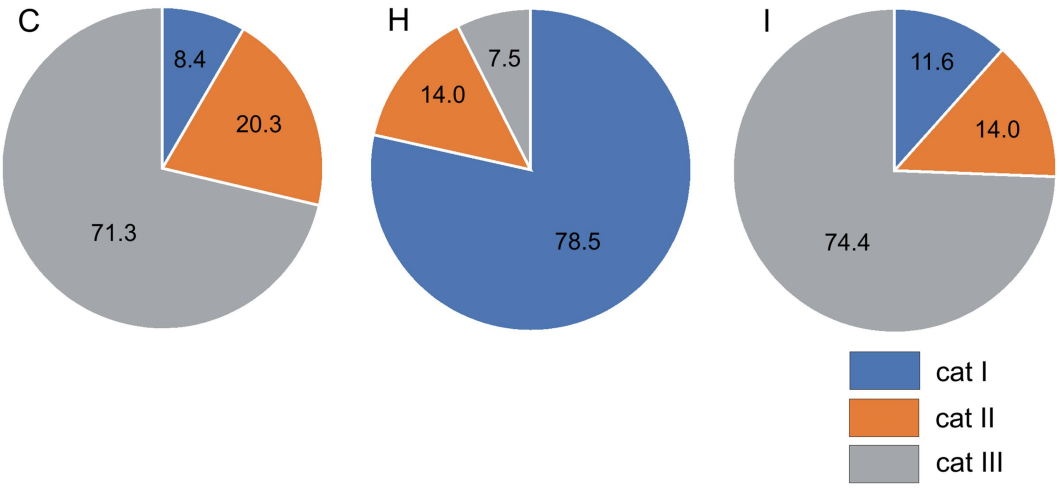

FIGURE 5
Incidence (%) of epicuticular wax categories outside the epistomatal area in different treatments (C – control, H – air humidification, I – soil irrigation).

to height growth over diameter growth in forest stands where light competition takes place (Falster and Westoby, 2003). This point is indirectly supported by the weaker impact of environmental factors on RGI dynamics in the second subperiod (Table 6). In addition, the increasing soil water content might be partly responsible for the decreased RGI during this period (Figure 1; Table 7). During the second and fourth periods, the SWC increased considerably, even in the control plots. Such a high SWC probably exceeds the

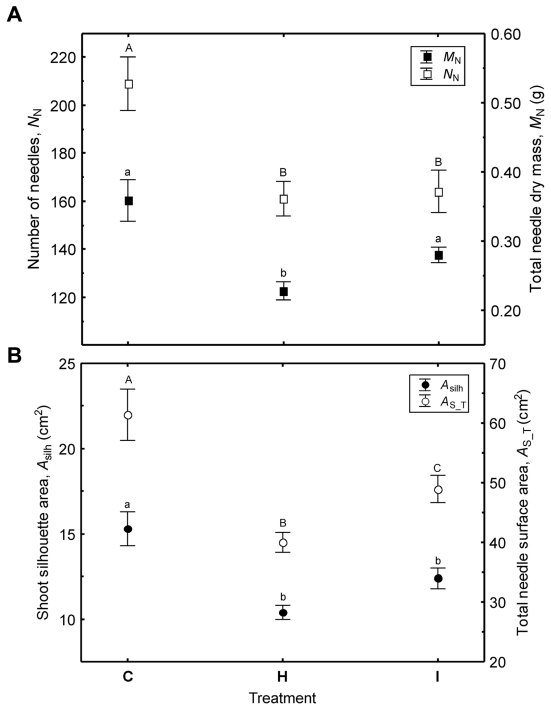

FIGURE 6
Variation of shoot size (mean ± SE) among the treatments (C – control, H – air humidification, I – soil irrigation): **(A)** – number of needles and total needle dry mass; **(B)** – shoot silhouette area and total needle surface area. Different letters denote significant ($p < 0.05$) differences between the treatments.

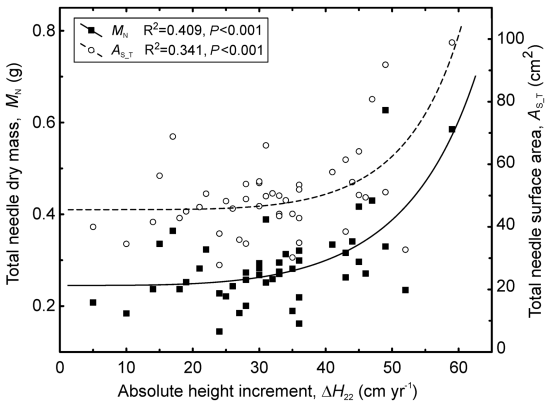

FIGURE 7
Relationships between shoot size (total needle dry mass and total needle surface area) and absolute height increment of stems (ΔH_{22}) across the treatments in 2022.

optimum for Norway spruce growth. It has been shown that Norway spruce is sensitive to both drought conditions (Haas et al., 2021; Luoranen et al., 2023) and water excess in topsoil (Glenz et al., 2006; Modrzyński, 2007). According to Niinemets and Valladares (2006), the index of waterlogging tolerance of *P. abies* is 1.22, i.e., very intolerant to intolerant. The very high soil water potential values in June suggest that the soil was likely saturated with water

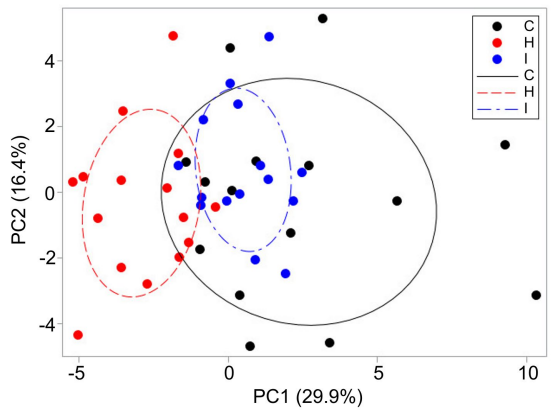

FIGURE 8
Distribution of sample trees ($n = 45$) among the humidity treatments (C – control, H – air humidification, I – soil irrigation) based on shoot and needle morphological traits according to PC1 and PC2. The ellipses include 50% of the data series observations.

(Table 1). In the soil of the FAHM site, the large size (> 50 µm) pores are filled with gravitational water above −6 kPa (Hansen et al., 2013). While the volume of air spaces in soil filled with gravitational water decreases considerably, the oxygen concentration in the soil declines. This might cause hypoxic conditions, aggravating nitrogen availability (Liang et al., 2023), development and functioning of the root system (Puhe, 2003; Kreuzwieser et al., 2009) and ultimately affecting tree growth.

The results of the current experiment suggest that *P. abies* trees growing under elevated air humidity exhibit a slower growth rate (H_T, ΔH_T, D_{30}) compared to the control trees growing under ambient conditions (Table 3). This growth response observed at northern latitudes is opposite that reported for Central Europe, where spruce growth is largely constrained by a high VPD (Trotsiuk et al., 2021; Etzold et al., 2022). However, our results are not exceptional. Also, in *Pinus koraiensis*, stem radial increments have been shown to be enhanced by a high ratio of actual to potential evapotranspiration, i.e., by high evaporative demand (Li et al., 2014). A similar growth response also occurred in fast-growing broadleaved species in the FAHM experiment (Sellin et al., 2017; Tullus et al., 2017; Oksanen et al., 2019). Our previous studies revealed several concurrent mechanisms potentially responsible for growth deceleration: impaired nutrient uptake resulting in reduced photosynthetic capacity; soil hypoxia inducing metabolic stress; retardation of foliar development; shifts in biomass allocation in favor of vascular tissues, leading to larger maintenance respiration costs; increase in proportion of living parenchyma cells in xylem, also enhancing stem respiration; reduced hydraulic conductance, limiting gas exchange in the case of weather extremes; and increasing risk of fungal damage. To ascertain the mechanisms behind the slowing down of growth in Norway spruce under conditions of increasing atmospheric humidity, further research is required. However, the current results demonstrate one common mechanism, the retardation of the development of assimilating surfaces, evidenced by the smaller size of the shoots, which is correlated with height increments. Destructive sampling of model trees in 2023 revealed significantly ($p < 0.01$) smaller total

foliar biomass in trees growing under elevated RH compared to the C and I treatments (K. Rosenvald, unpubl.). Our previous measurements at the FAHM experimental site indicated that a 5% increase in RH in an air layer a few meters thick does not affect the level of photosynthetically active radiation. The present study did not reveal significant shifts in nutrient uptake.

4.3 Future prospects in light of climate change

Picea abies is considered to be an adaptive specialist (Frank et al., 2017), meaning that the influence of the external environment has a significant impact on survival and physiological functions due to its sensitivity to changes in ecological factors. Although low genotype versus environment interactions refer to a high plasticity of Norway spruce, nevertheless it will be harder for the trees to adapt to climate change and higher temperatures in the future (Lundströmer et al., 2020). Sáenz-Romero et al. (2019) demonstrated lower resilience to climate change and stronger genetic clines in *P. abies*, which constrain its climate responses to narrower climatic ranges. In Central European forests, tree growth is mainly constrained by low temperatures at higher elevations, high VPD at mid-to low elevations and available soil water at low elevations, particularly toward the end of the growing season (Trotsiuk et al., 2021). The rising VPD induced by global warming will limit tree growth by replacing temperature constraints across large areas. However, our results suggest that the growth responses of *P. abies* to climate change are not uniform across its distribution area. At high latitudes, the increasing precipitation and concomitant rise in air humidity may counteract the enhancement of tree growth and forest productivity predicted for boreal forests due to global warming. The growth responses of *P. abies* differ between the phenological forms. The early-flushing trees exhibit higher growth rates, while late-flushing trees perform better under increasing environmental humidity. Given that the late phenological form is more tolerant of a wetter climate and is less threatened by late spring frosts, the potential for acclimation to regional climate trends is higher for the late phenological form.

Data availability statement

The raw data supporting the conclusions of this article will be made available by the authors, without undue reservation.

Author contributions

AS: Conceptualization, Formal analysis, Funding acquisition, Investigation, Project administration, Supervision, Writing – original draft, Writing – review & editing. KH: Formal analysis, Investigation, Methodology, Writing – original draft. PK: Formal analysis, Investigation, Methodology, Writing – original draft. RM: Investigation, Methodology, Writing – review & editing. EÕ-P: Formal analysis, Investigation, Writing – original draft. TR: Formal analysis, Investigation, Writing – original draft. KR: Data curation, Investigation, Writing – review & editing. AT: Formal analysis, Investigation, Methodology, Writing – original draft.

Funding

The author(s) declare that financial support was received for the research, authorship, and/or publication of this article. This work was supported by the Estonian Research Council grant PRG1434, the European Commission's Horizon 2020 program under grant agreement no. 101000406 (project ONEforest) and the AnaEE Estonia Project (2014–2020.4.01.20–0285) funded by the EU Regional Development Fund.

Acknowledgments

The authors are thankful to Urmas Lanto for operating the FAHM humidification system and to Märt Rahi for the scanning electron microscopy work.

Conflict of interest

The authors declare that the research was conducted in the absence of any commercial or financial relationships that could be construed as a potential conflict of interest.

Publisher's note

Supplementary material

The Supplementary material for this article can be found online at: https://www.frontiersin.org/articles/10.3389/ffgc.2024.1370934/full#supplementary-material

References

Arnič, D., Gričar, J., Jevšenak, J., Božič, G., von Arx, G., and Prislan, P. (2021). Different wood anatomical and growth responses in European beech (*Fagus sylvatica* L.) at three forest sites in Slovenia. *Front. Plant Sci.* 12:669229. doi: 10.3389/fpls.2021.669229

Barthlott, W., Neinhuis, C., Cutler, D., Ditsch, F., Meusel, I., Theisen, I., et al. (1998). Classification and terminology of plant epicuticular waxes. *Bot. J. Linn. Soc.* 126, 237–260. doi: 10.1111/j.1095-8339.1998.tb02529.x

Bartík, M., Jančo, M., Střelcová, K., Škvareninová, J., Škvarenina, J., Mikloš, M., et al. (2016). Rainfall interception in a disturbed montane spruce (*Picea abies*) stand in the West Tatra Mountains. *Biologia* 71, 1002–1008. doi: 10.1515/biolog-2016-0119

Bednář, P., Souček, J., Krejza, J., and Černý, J. (2022). Growth and morphological patterns of Norway spruce (*Picea abies* (L.) karst.) juveniles in response to light intensities. *Forests* 13:1804. doi: 10.3390/f13111804

Beier, C., Beierkuhnlein, C., Wohlgemuth, T., Penuelas, J., Emmett, B., Körner, C., et al. (2012). Precipitation manipulation experiments–challenges andrecommendations for the future. *Ecol. Lett.* 15, 899–911. doi: 10.1111/j.1461-0248.2012.01793.x

Betts, A. K., Desjardins, R., Worth, D., and Beckage, B. (2014). Climate coupling between temperature, humidity, precipitation, and cloud cover over the Canadian prairies. *J. Geophys. Res. Atmos.* 119, 13305–13326. doi: 10.1002/2014JD022511

Boisvert-Marsh, L., Périé, C., and de Blois, S. (2014). Shifting with climate? Evidence for recent changes in tree species distribution at high latitudes. *Ecosphere* 5, 1–33. doi: 10.1890/ES14-00111.1

Bolton, D. (1980). The computation of equivalent potential temperature. *Mon. Weather Rev.* 108, 1046–1053. doi: 10.1175/1520-0493(1980)108<1046:TCOEPT>2.0.CO;2

Bonan, G. B. (2010). *Ecological climatology. Concepts and applications*. Cambridge: Cambridge University Press.

Bradshaw, R. H. W., Holmqvist, B. H., Cowling, S. A., and Sykes, M. T. (2000). The effects of climate change on the distribution and management of *Picea abies* in southern Scandinavia. *Can. J. For. Res.* 30, 1992–1998. doi: 10.1139/x00-130

Busuioc, A., Birsan, M.-V., Carbunaru, D., Baciu, M., and Orzan, A. (2016). Changes in the large-scale thermodynamic instability and connection with rain shower frequency over Romania: verification of the Clausius–Clapeyron scaling. *Int. J. Climatol.* 36, 2015–2034. doi: 10.1002/joc.4477

Byrne, M. P., and O'Gorman, P. A. (2018). Trends in continental temperature and humidity directly linked to ocean warming. *Proc. Natl. Acad. Sci. USA* 115, 4863–4868. doi: 10.1073/pnas.1722312115

Dessler, A. E., and Davis, S. M. (2010). Trends in tropospheric humidity from reanalysis systems. *J. Geophys. Res.* 115:D19127. doi: 10.1029/2010JD014192

Diffenbaugh, N. S., and Field, C. B. (2013). Changes in ecologically critical terrestrial climate conditions. *Science* 341, 486–492. doi: 10.1126/science.1237123

Esch, A., and Mengel, K. R. (1998). Combined effects of acid mist and frost drought on the water status of young spruce trees (*Picea abies*). *Environ. Exp. Bot.* 39, 57–65. doi: 10.1016/S0098-8472(97)00035-X

Etverk, I. (1968). "Hariliku kuuse fenoloogilistest vormidest" in *Eesti Põllumajanduse Akadeemia teaduslike tööde kogumik, kd. 50*. ed. K. Veermets (Tartu: EPA), 105–120.

Etzold, S., Sterck, F., Bose, A. K., Braun, S., Buchmann, N., Eugster, W., et al. (2022). Number of growth days and not length of the growth period determines radial stem growth of temperate trees. *Ecol. Lett.* 25, 427–439. doi: 10.1111/ele.13933

European Environment Agency. (2016). *Climate change, impacts and vulnerability in Europe. An Indicator-based report. EAA report no 1/2017*. Copenhagen: European Environment Agency.

Falster, D. S., and Westoby, M. (2003). Plant height and evolutionary games. *Trends Ecol. Evol.* 18, 337–343. doi: 10.1016/S0169-5347(03)00061-2

Fanourakis, D., Aliniaeifard, S., Sellin, A., Giday, H., Körner, O., Rezaei Nejad, A., et al. (2020). Stomatal behavior following mid-or long-term exposure to high relative air humidity: a review. *Plant Physiol. Biochem.* 153, 92–105. doi: 10.1016/j.plaphy.2020.05.024

Frank, A., Sperisen, C., Howe, G. T., Brang, P., and Walthert, L. (2017). Distinct genecological patterns in seedlings of Norway spruce and silver fir from a mountainous landscape. *Ecology* 98, 211–227. doi: 10.1002/ecy.1632

Gebauer, R., Volarík, D., Urban, J., Børja, I., Nagy, N. E., Eldhuset, T. D., et al. (2019). Effects of mild drought on the morphology of sun and shade needles in 20-year-old Norway spruce trees. *iForest* 12, 27–34. doi: 10.3832/ifor2809-011

Geiger, R., Aron, R. H., and Todhunter, P. (2009). *The climate near the ground*. Lanham: Rowman and Littlefield.

Glenz, C., Schlaepfer, R., Iorgulescu, I., and Kienast, F. (2006). Flooding tolerance of central European tree and shrub species. *For. Ecol. Manag.* 235, 1–13. doi: 10.1016/j.foreco.2006.05.065

Godbold, D., Tullus, A., Kupper, P., Sõber, J., Ostonen, I., Godbold, J. A., et al. (2014). Elevated atmospheric CO_2 and humidity delay leaf fall in *Betula pendula*, but not in *Alnus glutinosa* or *Populus tremula*×*tremuloides*. *Ann. For. Sci.* 71, 831–842. doi: 10.1007/s13595-014-0382-4

Grassi, G., and Giannini, R. (2005). Influence of light and competition on crown and shoot morphological parameters of Norway spruce and silver fir saplings. *Ann. For. Sci.* 62, 269–274. doi: 10.1051/forest:2005019

Haas, J. C., Vergara, A., Serrano, A. R., Mishra, S., Hurry, V., and Street, N. R. (2021). Candidate regulators and target genes of drought stress in needles and roots of Norway spruce. *Tree Physiol.* 41, 1230–1246. doi: 10.1093/treephys/tpaa178

Hansen, R., Mander, Ü., Soosaar, K., et al (2013). Greenhouse gas fluxes in an open air humidity manipulation experiment. *Landscape Ecol.* 28, 637–649.

Hejnowicz, A. (2007). "Anatomy, embryology, and karyology" in *Biology and ecology of Norway spruce*. eds. M. G. Tjoelker, A. Boratyński and W. Bugała, vol. *78* (Dordrecht: Springer), 49–70.

IPCC (2021). "Climate change 2021: The physical science basis" in *Contribution of working group I to the sixth assessment report of the intergovernmental panel on climate change*. ed. V. Masson-Delmotte (Cambridge: Cambridge University Press)

Ishii, H., Hamada, Y., and Utsugi, H. (2012). Variation in light-intercepting area and photosynthetic rate of sun and shade shoots of two Picea species in relation to the angle of incoming light. *Tree Physiol.* 32, 1227–1236.

Jung, M., Reichstein, M., Ciais, P., Seneviratne, S. I., Sheffield, J., Goulden, M. L., et al. (2010). Recent decline in the global land evapotranspiration trend due to limited moisture supply. *Nature* 467, 951–954. doi: 10.1038/nature09396

Keenan, T. F., Gray, J., Friedl, M. A., Toomey, M., Bohrer, G., Hollinger, D. Y., et al. (2014). Net carbon uptake has increased through warming-induced changes in temperate forest phenology. *Nat. Clim. Chang.* 4, 598–604. doi: 10.1038/nclimate2253

Kivimäenpää, M., Riikonen, J., Ahonen, V., Tervahauta, A., and Holopainen, T. (2013). Sensitivity of Norway spruce physiology and terpenoid emission dynamics to elevated ozone and elevated temperature under open-field exposure. *Environ. Exp. Bot.* 90, 32–42. doi: 10.1016/j.envexpbot.2012.11.004

Kivimäenpää, M., Sutinen, S., Valolahti, H., Häikiö, E., Riikonen, J., Kasurinen, A., et al. (2017). Warming and elevated ozone differently modify needle anatomy of Norway spruce (*Picea abies*) and scots pine (*Pinus sylvestris*). *Can. J. For. Res.* 47, 488–499. doi: 10.1139/cjfr-2016-0406

Koch, O., de Avila, A. L., Heinen, H., and Albrecht, A. T. (2022). Retreat of major European tree species distribution under climate change—minor natives to the rescue? *Sustain. For.* 14:5213. doi: 10.3390/su14095213

Koppel, A., and Heinsoo, K. (1996). Epicuticular wax structure of Norway spruce (*Picea abies*) needles in Estonia. Variability in naturally growing and cloned trees. *Ann. Bot. Fenn.* 33, 265–273.

Kreuzwieser, J., Hauberg, J., Howell, K. A., Carroll, A., Rennenberg, H., Millar, A. H., et al. (2009). Differential response of gray poplar leaves and roots underpins stress adaptation during hypoxia. *Plant Physiol.* 149, 461–473. doi: 10.1104/pp.108.125989

Kupper, P., Sõber, J., Sellin, A., Lõhmus, K., Tullus, A., Räim, O., et al. (2011). An experimental facility for free air humidification manipulation (FAHM) can alter water flux through deciduous tree canopy. *Environ. Exp. Bot.* 72, 432–438. doi: 10.1016/j.envexpbot.2010.09.003

le Provost, G., Domergue, F., Lalanne, C., Ramos Campos, P., Grosbois, A., Bert, D., et al. (2013). Soil water stress affects both cuticular wax content and cuticle-related gene expression in young saplings of maritime pine (*Pinus pinaster* Ait). *BMC Plant Biol.* 13:95. doi: 10.1186/1471-2229-13-95

Lendzion, J., and Leuschner, C. (2008). Growth of European beech (Fagus sylvatica L.) saplings is limited by elevated atmospheric vapour pressure deficits. *For. Ecol. Manage.* 256, 648–655.

Leuschner, C., and Lendzion, J. (2009). Air humidity, soil moisture and soil chemistry as determinants of the herb layer composition in European beech forests. *J. Veg. Sci.* 20, 288–298.

Li, G., Harrison, S. P., Prentice, I. C., and Falster, D. (2014). Simulation of tree-ring widths with a model for primary production, carbon allocation, and growth. *Biogeosciences* 11, 6711–6724. doi: 10.5194/bg-11-6711-2014

Liang, M., Sugimoto, A., Tei, S., Takano, S., Morozumi, T., Shingubara, R., et al. (2023). Arctic plant responses to summer climates and flooding events: a study of carbon and nitrogen-related larch growth and ecosystem parameters in northeastern Siberia. *J. Geophys. Res. Biogeosci.* 128:e2022JG007135. doi: 10.1029/2022JG007135

Lindner, M., Fitzgerald, J. B., Zimmermann, N. E., et al (2014). Climate change and European forests: What do we know, what are the uncertainties, and what are the implications for forest management? *J. Environ. Manage.* 146, 69–83.

Liu, Y., Parolari, A. J., Kumara, M., Huang, C.-W., Katul, G. G., and Porporato, A. (2017). Increasing atmospheric humidity and CO_2 concentration alleviate forest mortality risk. *Proc. Natl. Acad. Sci. USA* 114, 9918–9923. doi: 10.1073/pnas.1704811114

Luhamaa, A., Kallis, A., Mändla, K., Männik, A., Pedusaar, T., and Rosin, K. (2015). *Eesti tuleviku kliimastsenaariumid aastani 2100*. Tallinn: Keskkonnaagentuur.

Lundströmer, J., Karlsson, B., and Berlin, M. (2020). Strategies for deployment of reproductive material under supply limitations – a case study of Norway spruce seed sources in Sweden. *Scand. J. For. Res.* 35, 495–505. doi: 10.1080/02827581.2020.1833979

Luoranen, J., Riikonen, J., and Saksa, T. (2023). Damage caused by an exceptionally warm and dry early summer on newly planted Norway spruce container seedlings in Nordic boreal forests. *For. Ecol. Manag.* 528:120649. doi: 10.1016/j.foreco.2022.120649

Luyssaert, S., Marie, G., Valade, A., Chen, Y. Y., Njakou Djomo, S., Ryder, J., et al. (2018). Trade-offs in using European forests to meet climate objectives. *Nature* 562, 259–262. doi: 10.1038/s41586-018-0577-1

Mäkinen, H., Jyske, T., and Nöjd, P. (2018). Dynamics of diameter and height increment of Norway spruce and scots pine in southern Finland. *Ann. For. Sci.* 75:28. doi: 10.1007/s13595-018-0710-1

Mäkinen, H., Nöjd, P., and Isomäki, A. (2002). Radial, height and volume increment variation in *Picea abies* (L.) karst. Stands with varying thinning intensities. *Scand. J. For. Res.* 17, 304–316. doi: 10.1080/02827580260138062

Mäkinen, H., Nöjd, P., and Mielikäinen, K. (2000). Climatic signal in annual growth variation of Norway spruce (*Picea abies* (L.) karst.) along a transect from Central Finland to Arctic timberline. *Can. J. For. Res.* 30, 769–777. doi: 10.1139/x00-005

Marozas, V., Augustaitis, A., Pivoras, A., Baumgarten, M., Mozgeris, G., Sasnauskienė, J., et al. (2019). Comparative analyses of gas exchange characteristics and

chlorophyll fluorescence of three dominant tree species during the vegetation season in hemi-boreal zone, Lithuania. *J. Agric. Meteorol.* 75, 3–12. doi: 10.2480/agrmet.D-18-00004

Matějka, K., Leugner, J., and Krpeš, V. (2014). Phenotype features in juvenile populations of *Picea abies* and their growth. *J. For. Sci.* 60, 96–108. doi: 10.17221/77/2013-JFS

Matula, R., Knířová, S., Vítámvás, J., Šrámek, M., Knít, T., Ulbrichová, I., et al. (2023). Shifts in intra-annual growth dynamics drive a decline in productivity of temperate trees in central European forest under warmer climate. *Sci. Total Environ.* 905:166906. doi: 10.1016/j.scitotenv.2023.166906

McDowell, N. G., and Allen, C. D. (2015). Darcy's law predicts widespread forest mortality under climate warming. *Nat. Clim. Chang.* 5, 669–672. doi: 10.1038/nclimate2641

Menzel, A., Sparks, T. H., Estrella, N., Koch, E., Aasa, A., Ahas, R., et al. (2006). European phenological response to climate change matches the warming pattern. *Glob. Chang. Biol.* 12, 1969–1976. doi: 10.1111/j.1365-2486.2006.01193.x

Modrzyński, J. (2007). "Outline of ecology" in *Biology and ecology of Norway spruce*. eds. M. G. Tjoelker, A. Boratyński and W. Bugała, vol. *78* (Dordrecht: Springer), 195–221.

Neuner, S., Albrecht, A., Cullmann, D., Engels, F., Griess, V. C., Hahn, W. A., et al. (2015). Survival of Norway spruce remains higher in mixed stands under a dryer and warmer climate. *Glob. Change Biol.* 21, 935–946. doi: 10.1111/gcb.12751

Niinemets, Ü., and Kull, O. (1995). Effects of light availability and tree size on the architecture of assimilative surface in the canopy of *Picea abies*: variation in shoot structure. *Tree Physiol.* 15, 791–798. doi: 10.1093/treephys/15.12.791

Niinemets, Ü., and Valladares, F. (2006). Tolerance to shade, drought, and waterlogging of temperate northern hemisphere trees and shrubs. *Ecol. Monogr.* 76, 521–547. doi: 10.1890/0012-9615(2006)076[0521:TTSDAW]2.0.CO;2

Oksanen, E., Lihavainen, J., Keinänen, M., Keski-Saari, S., Kontunen-Soppela, S., and Sellin, A. (2019). Northern forest trees under increasing atmospheric humidity. *Prog. Bot.* 80, 317–336. doi: 10.1007/124_2017_15

Palmroth, S., Stenberg, P., Smolander, S., Voipio, P., and Smolander, H. (2002). Fertilization has little effect on light-interception efficiency of *Picea abies* shoots. *Tree Physiol.* 22, 1185–1192. doi: 10.1093/treephys/22.15-16.1185

Park Williams, A., Allen, C. D., Macalady, A. K., Griffin, D., Woodhouse, C. A., Meko, D. M., et al. (2013). Temperature as a potent driver of regional forest drought stress and tree mortality. *Nat. Clim. Change* 3, 292–297. doi: 10.1038/nclimate1693

Perrin, M., Rossi, S., and Isabel, N. (2017). Synchronisms between bud and cambium phenology in black spruce: early-flushing provenances exhibit early xylem formation. *Tree Physiol.* 37, 593–603. doi: 10.1093/treephys/tpx019

Petr, M., Boerboom, L. G. J., Ray, D., and van der Veen, A. (2015). Adapting Scotland's forests to climate change using an action expiration chart. *Environ. Res. Lett.* 10:105005. doi: 10.1088/1748-9326/10/10/105005

Popović, V., Nikolić, B., Lučić, A., Rakonjac, L., Jovanović, D. Š., and Miljković, D. (2022). Morpho-anatomical trait variability of the Norway spruce (*Picea abies* (L.) karst.) needles in natural populations along elevational diversity gradient. *Trees* 36, 1131–1147. doi: 10.1007/s00468-022-02277-1

Pudas, E., Leppälä, M., Tolvanen, A., Poikolainen, J., Venäläinen, A., and Kubin, E. (2008). Trends in phenology of *Betula pubescens* across the boreal zone in Finland. *Int. J. Biometeorol.* 52, 251–259. doi: 10.1007/s00484-007-0126-3

Puhe, J. (2003). Growth and development of the root system of Norway spruce (*Picea abies*) in forest stands—a review. *For. Ecol. Manag.* 175, 253–273. doi: 10.1016/S0378-1127(02)00134-2

R Core Team. (2018). *R: A language and environment for statistical computing*. Vienna, Austria: R Foundation for Statistical Computing.

Reich, P. B., Bermudez, R., Montgomery, R. A., Rich, R. L., Rice, K. E., Hobbie, S. E., et al. (2022). Even modest climate change may lead to major transitions in boreal forests. *Nature* 608, 540–545. doi: 10.1038/s41586-022-05076-3

Sáenz-Romero, C., Kremer, A., Nagy, L., Újvári-Jármay, É., Ducousso, A., Kóczán-Horváth, A., et al. (2019). Common garden comparisons confirm inherited differences in sensitivity to climate change between forest tree species. *PeerJ* 7:e6213. doi: 10.7717/peerj.6213

Šantrůček, J. (2022). The why and how of sunken stomata: does the behaviour of encrypted stomata and the leaf cuticle matter? *Ann. Bot.* 130, 285–300. doi: 10.1093/aob/mcac055

Scoccimarro, E., Villarini, G., Vichi, M., Zampieri, M., Fogli, P. G., Bellucci, A., et al. (2015). Projected changes in intense precipitation over Europe at the daily and subdaily time scales. *J. Clim.* 28, 6193–6203. doi: 10.1175/JCLI-D-14-00779.1

Sellin, A. (2000). Estimating the needle area from geometric measurements: application of different calculation methods to Norway spruce. *Trees* 14, 215–222. doi: 10.1007/PL00009765

Sellin, A. (2001). Morphological and stomatal responses of Norway spruce foliage to irradiance within a canopy depending on shoot age. *Environ. Exp. Bot.* 45, 115–131. doi: 10.1016/S0098-8472(00)00086-1

Sellin, A., Alber, M., Keinänen, M., Kupper, P., Lihavainen, J., Lõhmus, K., et al. (2017). Growth of northern deciduous trees under increasing atmospheric humidity: possible mechanisms behind the growth retardation. *Reg. Environ. Chang.* 17, 2135–2148. doi: 10.1007/s10113-016-1042-z

Škvareninová, J., and Mrekaj, I. (2022). Impact of climate change on Norway spruce flowering in the southern part of the Western Carpathians. *Front. Ecol. Evol.* 10:865471. doi: 10.3389/fevo.2022.865471

Šrámek, V., Neudertová Hellebrandová, K., and Fadrhonsová, V. (2019). Interception and soil water relation in Norway spruce stands of different age during the contrasting vegetation seasons of 2017 and 2018. *J. For. Sci.* 65, 51–60. doi: 10.17221/135/2018-JFS

Stenberg, P., Kangas, T., Smolander, H., and Linder, S. (1999). Shoot structure, canopy openness, and light interception in Norway spruce. *Plant Cell Environ.* 22, 1133–1142.

Stenberg, P., Palmroth, S., Bond, B. J., Sprugel, D. G., and Smolander, H. (2001). Shoot structure and photosynthetic efficiency along the light gradient in a scots pine canopy. *Tree Physiol.* 21, 805–814. doi: 10.1093/treephys/21.12-13.805

Trimbacher, C., and Egkmüllner, O. (1997). A method for quantifying changes in the epicuticular wax structure of Norway spruce needles. *Eur. J. For. Path.* 27, 83–93. doi: 10.1111/j.1439-0329.1997.tb01359.x

Trotsiuk, V., Babst, F., Grossiord, C., Gessler, A., Forrester, D. I., Buchmann, N., et al. (2021). Tree growth in Switzerland is increasingly constrained by rising evaporative demand. *J. Ecol.* 109, 2981–2990. doi: 10.1111/1365-2745.13712

Tullus, A., Kupper, P., Kaasik, A., Tullus, H., Lõhmus, K., Sõber, A., et al. (2017). The competitive status of trees determines their responsiveness to increasing atmospheric humidity – a climate trend predicted for northern latitudes. *Glob. Change Biol.* 23, 1961–1974. doi: 10.1111/gcb.13540

Tuomisto, H. (1988). Use of *Picea abies* needles as indicators of air pollution: epicuticular wax morphology. *Ann. Bot. Fenn.* 25, 351–364.

Utkina, I. A., and Rubtsov, V. V. (2017). Studies of phenological forms of pedunculate oak. *Contemp. Probl. Ecol.* 10, 804–811. doi: 10.1134/S1995425517070101

Venäläinen, A., Lehtonen, I., Laapas, M., Ruosteenoja, K., Tikkanen, O. P., Viiri, H., et al. (2020). Climate change induces multiple risks to boreal forests and forestry in Finland: a literature review. *Glob. Change Biol.* 26, 4178–4196. doi: 10.1111/gcb.15183

Vicente-Serrano, S. M., Nieto, R., Gimeno, L., Azorin-Molina, C., Drumond, A., el Kenawy, A., et al. (2018). Recent changes of relative humidity: regional connections with land and ocean processes. *Earth Syst. Dynam.* 9, 915–937. doi: 10.5194/esd-9-915-2018

von Arx, G., Dobbertin, M., and Rebetez, M. (2012). Spatio-temporal effects of forest canopy on understory microclimate in a long-term experiment in Switzerland. *Agric. For. Meteorol.* 166-167, 144–155. doi: 10.1016/j.agrformet.2012.07.018

Wang, M. H., Wang, J. R., Zhang, X. W., Zhang, A. P., Sun, S., and Zhao, C. M. (2019). Phenotypic plasticity of stomatal and photosynthetic features of four *Picea* species in two contrasting common gardens. *AoB Plants* 11:plz034. doi: 10.1093/aobpla/plz034

Xiao, M., Yu, Z., Kong, D., Gu, X., Mammarella, I., Montagnani, L., et al. (2020). Stomatal response to decreased relative humidity constrains the acceleration of terrestrial evapotranspiration. *Environ. Res. Lett.* 15:094066. doi: 10.1088/1748-9326/ab9967

Zhang, J., Jiang, H., Song, X., Jin, J., and Zhang, X. (2018). The responses of plant leaf CO_2/H_2O exchange and water use efficiency to drought: a meta-analysis. *Sustain. For.* 10:551. doi: 10.3390/su10020551

Zhu, J., Thimonier, A., Etzold, S., Meusburger, K., Waldner, P., Schmitt, M., et al. (2022). Variation in leaf morphological traits of European beech and Norway spruce over two decades in Switzerland. *Front. For. Glob. Change* 4:778351. doi: 10.3389/ffgc.2021.778351